Received: 13 March 2020 | Revised: 31 August 2020 | Accepted: 2 September 2020

DOI: 10.1002/hyp.13909

RESEARCH ARTICLE

WILEY

Comparison of environmental tracers including organic micropollutants as groundwater exfiltration indicators into a small river of a karstic catchment

Clarissa Glaser[1] | Marc Schwientek[1] | Tobias Junginger[2] | Benjamin Silas Gilfedder[3] | Sven Frei[4] | Martina Werneburg[1] | Christian Zwiener[1] | Christiane Zarfl[1]

[1]Center for Applied Geoscience, Eberhard Karls University of Tübingen, Tübingen, Germany

[2]Laboratoire d'Hydrologie et de Géochimie de Strasbourg (LHyGeS), Université de Strasbourg/ENGEES, Strasbourg, France

[3]Limnological Research Station, Bayreuth Center of Ecology and Environmental Research (BAYCEER), University of Bayreuth, Bayreuth, Germany

[4]Department of Hydrology, Bayreuth Center of Ecology and Environmental Research (BAYCEER), University of Bayreuth, Bayreuth, Germany

Correspondence
Clarissa Glaser, Center for Applied Geoscience, Eberhard Karls University of Tübingen, Tübingen, Germany.
Email: clarissa.glaser@uni-tuebingen.de

Funding information
German Research Foundation (DFG), Grant/Award Number: SFB 1253/1 2017

Abstract

Understanding groundwater–surface water (GW–SW) interactions is vital for water management in karstic catchments due to its impact on water quality. The objective of this study was to evaluate and compare the applicability of seven environmental tracers to quantify and localize groundwater exfiltration into a small, human-impacted karstic river system. Tracers were selected based on their emission source to the surface water either as (a) dissolved, predominantly geogenic compounds (radon-222, sulphate and electrical conductivity) or (b) anthropogenic compounds (predominantly) originating from wastewater treatment plant (WWTP) effluents (carbamazepine, tramadol, sodium, chloride). Two contrasting sampling approaches were compared (a) assuming steady-state flow conditions and (b) considering the travel time of the water parcels (Lagrangian sampling) through the catchment to account for diurnal changes in inflow from the WWTP. Spatial variability of the concentrations of all tracers indicated sections of preferential groundwater inflow. Lagrangian sampling techniques seem highly relevant for capturing dynamic concentration patterns of WWTP-derived compounds. Quantification of GW inflow with the finite element model FINIFLUX, based on observed in-stream Rn activities led to plausible fluxes along the investigated river reaches (0.265 m^3 s^{-1}), while observations of other natural or anthropogenic environmental tracers produced less plausible water fluxes. Important point sources of groundwater exfiltration can be ascribed to locations where the river crosses geological fault lines. This indicates that commonly applied concepts describing groundwater–surface water interactions assuming diffuse flow in porous media are difficult to transfer to karstic river systems whereas concepts from fractured aquifers may be more applicable. In general, this study helps selecting the best suited hydrological tracer for GW exfiltration and leads to a better understanding of processes controlling groundwater inflow into karstic river systems.

KEYWORDS

carbamazepine, groundwater inflow, Lagrangian sampling, radon, wastewater treatment plant, water quality

1 | INTRODUCTION

Groundwater (GW) and surface water (SW) are coupled reservoirs with complex exchange processes that influence both systems (Atkinson et al., 2015; Cook, 2013; Gilfedder, Frei, Hofmann, & Cartwright, 2015). In rivers, water and matter fluxes between these compartments play an important role for the water availability, water quality and ecology and are thus relevant processes to be considered for sustainable water management (Brunke & Gonser, 1997). Existing methods that aim to characterize and quantify interactions between GW and SW are diverse and were reviewed in detail by Kalbus, Reinstorf, and Schirmer (2006). Water flux measurements include, among others, for example, seepage meters (Fryar, Wallin, & Brown, 2000; Lee, 1977) or incremental streamflow discharge measurements (Payn, Gooseff, McGlynn, Bencala, & Wondzell, 2009).

During the past decades, environmental tracers have been used for quantification of local GW inflows to rivers and streams. GW inflows can be observed at a high spatial resolution and instrumentation costs are, depending on the tracer, often low (Cook, 2013). Measurements of environmental isotopic tracers such as the isotopes of hydrogen and oxygen in water (Oxtobee & Novakowski, 2002), radon (Frei & Gilfedder, 2015; Unland et al., 2013) and strontium (Harrington, Gardner, & Munday, 2014) are applied for this purpose, as well as measurements of ions (Smith, Pollock, & Palmer, 2010) or electrical conductivity (Oxtobee & Novakowski, 2002). For the successful application of these environmental tracers, two main underlying conditions must be met: (a) GW and river water must be significantly and measurably different in their concentrations (so-called endmember concentrations due to their 'endpoint character' in a two component mixing concept), and (b) GW endmember concentrations must be homogeneously distributed within the investigated region or the variability of endmember concentration must be known. Ions and electrical conductivity (EC) were used for the characterization of GW inflows where geological settings lead to a prominent difference in concentrations between GW and SW (Atkinson et al., 2015). EC mass balances describing GW inflows were applied for ~~a~~ different ecosystems all over the world (Gilfedder et al., 2015; Oxtobee & Novakowski, 2002; Smith et al., 2010). Also sodium and chloride were used extensively for the characterization of GW–SW interactions (Atkinson et al., 2015; Cartwright & Gilfedder, 2015; Cartwright, Hofmann, Sirianos, Weaver, & Simmons, 2011; Kumar, Ramanathan, & Keshari, 2009; Yang et al., 2012; Yu, L, Cartwright, Braden, & de Bree, 2013). In recent investigations, radon (^{222}Rn) has been increasingly applied due to the large concentration difference between groundwater and river water as well as its chemical properties (Avery, Bibby, Visser, Esser, & Moran, 2018; Cook, 2013; Cook, Rodellas, & Stieglitz, 2018; Zhao et al., 2018). Radon-222 is an inert noble gas of the ^{238}Uranium decay chain and characterized by an accumulation in the aquifer depending on chemical composition, mineralogy and lithology. Higher activities in GW, but a fast radioactive decay (half-life of 3.8 days) and loss to the atmosphere in SW maintain the large activity difference between these compartments (1–3 orders of magnitude). In general, multiple tracer approaches and a combination of different techniques reduce uncertainties in the quantification and, perhaps more importantly, allow uncertainty to be quantified (Avery et al., 2018; Zhao et al., 2018).

Globally, rivers and streams are affected by anthropogenic inputs of organic (micro)pollutants (Malaj et al., 2014; Schwarzenbach et al., 2006). The main emission pathway of majority of organic micropollutants into SWs are wastewater treatment plants (WWTP; Gros, Petrović, & Barceló, 2007). Continuous improvements in analytical methods have allowed the detection of organic micropollutants even at low concentrations (Clara, Strenn, & Kreuzinger, 2004). Despite the known negative influence of these compounds on freshwater ecosystems such as toxicological effects on biological systems, they also can be used for scientific purposes: Persistent organic micropollutants may be suitable tracers to better understand and characterize hydrological processes (Clara et al., 2004). Organic micropollutant concentrations (sulfamethoxazole, carbamazepine, ibuprofen) were used as anthropogenic indicators in the hyporheic zone (Banzhaf, Krein, & Scheytt, 2012) and to understand GW–SW interactions in a lowland Chalk catchment (Manamsa, Lapworth, & Stuart, 2016). A prominent example is carbamazepine which is often considered conservative due to its long half-life compared to the travel time of river water (Guillet et al., 2019; Kunkel & Radke, 2012; Pal, Gin, Lin, & Reinhard, 2010; Schwientek, Guillet, Rügner, Kuch, & Grathwohl, 2016). The persistent behaviour of a selected compound is indispensable for its successful application as a tracer, but the persistence may be river-specific. The analgesic tramadol for example was described to undergo attenuation processes in a river (Li, Sobek, & Radke, 2016), whereas other studies indicate a conservative character(e.g., Glaser et al., 2020). Concentrations of WWTP-derived compounds in small rivers often show a diurnal signal due to changing discharge from the WWTP (Schwientek et al., 2016). To distinguish advection of the transient concentration signal from actual loss processes, Lagrangian sampling is necessary for the quantification of processes affecting pollutant fluxes and concentrations. This sampling technique aims at the repeated sampling of the same water parcel as it moves downstream to follow the advective (and dispersive) transport of the pollutant within this water parcel and thus enable a comparison of pollutant concentrations with regard to potential loss processes.

Despite the general suitability of specific organic micropollutants for studying water exchange between GW and rivers, localization and quantification of GW inflow has not been conducted yet with these compounds. In addition, tracer-based quantification of the GW inflow has, so far, focussed on river systems with little anthropogenic influence and predominantly in rivers embedded in geologically porous media. This is due to the complexity of karstic aquifers (Bittner, Narany, Kohl, Disse, & Chiogna, 2018) that leads to hardly comparable subsurface water flow, transport and storage mechanisms in comparison to porous aquifers (Dvory et al., 2018; Hartmann & Baker, 2017). Previous field-based studies have focused on the interaction between karstic rock aquifers and rivers by applying hydraulic head measurements (Bailly-Comte, Jourde, & Pistre, 2009) or artificial tracers (Barberá & Andreo, 2017). To date, it is still not fully understood how

the connection between a catchment and its receiving river works hydrologically, that is, via which flow paths and processes the runoff from the catchment area drains into the river network. This is of particular interest also in the special case of karst landscapes. We hypothesize that in human-impacted catchments substances that are emitted via the WWTP might be a suitable tool to close this research gap. Therefore, the aim of this study was (a) to investigate the applicability of environmental tracers in a river (Ammer River, Southwest Germany) that is embedded in a karstic geology by a spatially high resolution approach and (b) to validate the reliability of seven different environmental tracers including selected conservative organic micropollutants for the quantification of GW inflow. To this end, a river segment which is generally assumed to drain the karst system, that is, with a groundwater flux towards the river and without known water losses to the underground, was selected.

2 | MATERIALS AND METHODS

2.1 | Sampling site

The Ammer catchment is located in Southwestern Germany and has an area of 238 km^2 (Figure 1a). The catchment is characterized by agricultural land use (50%), urban areas (12%) and managed forest (38%). The average discharge (Q) from the gauged catchment in Pfäffingen (134 km^2) is 0.87 m^3 s^{-1}. It is a tributary (fifth order stream) of the Neckar River with a total length of 22 km. The WWTP Gäu-Ammer [WWTP (1); 80,000 person equivalent (PE)] releases its treated sewage at the left river bank (flow direction) into the Ammer River. The mean dry weather effluent flow rate from the WWTP is 0.10–0.12 m^3 s^{-1}. Further details on WWTP flow during the sampling period can be found in Glaser et al. (2020). A 5,880 m long river reach downstream of the WWTP was selected for our investigations (Figure 2) where a distance of 0 m denotes the most upstream sampling location. In this section, the riverbed consists of larger cobbles with gravel and mainly silty material in the interstitial spaces. The average slope of the streambed for this reach is ~4‰. The two main tributaries are the Kochhart and the Käsbach creeks. A second WWTP is located at the Kochhart [WWTP (2); Hailfingen, 9,000 PE]. The selected river reach has an altered character due to its straightened channel (Figure S1), two constructed diversions in Reusten (length diversion 320 m) and Poltringen (length diversion 200 m), respectively, and two weirs for former mills. Many tributaries are tile drains that carry small amounts of water (0.005–0.015 m^3 s^{-1}) and discharge into the Ammer in pipes. A drinking water treatment plant processing groundwater (Carix method; ion exchange procedure water softening) discharges a pulsed water flow into the Ammer River (six times per day, in total 83 m^3, on 18 June 2018; transferable to other days during the sampling campaign).

The geology is dominated by karstic limestones of the Middle Triassic ('Muschelkalk') which form an important regional aquifer. The limestone crops out in the northwest and dips at 1–2° to the southwest. In this direction, it is increasingly covered by claystones and evaporites of the Upper Triassic ('Keuper') which are, in the gypsum bearing parts, also karstified ('Gipskeuper'). 'Muschelkalk' dominates in the upper ~4.3 km of the investigation reach (Selle, Schwientek, &

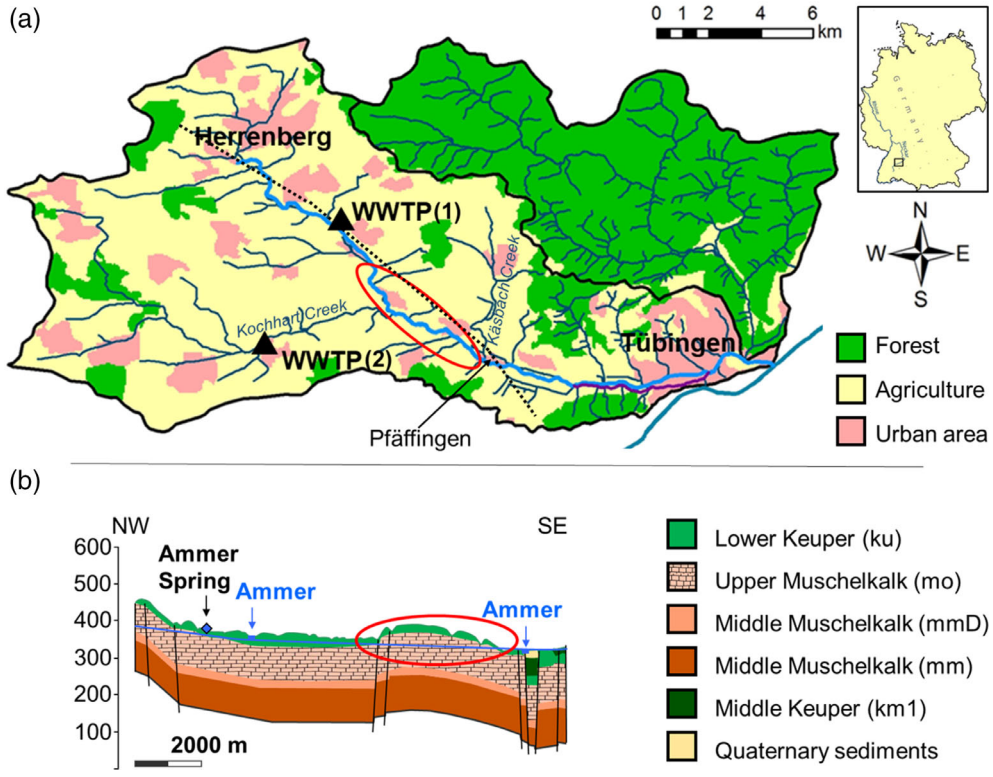

FIGURE 1 Graphical overview of the Ammer catchment (a) with locations of the wastewater treatment plants at the main stem (WWTP 1) and at the tributary Kochhart Creek (WWTP 2), as well as the investigation area (red circle; (a) and (b)). The dotted line of (a) highlights the location of the geological profile (b) that is mostly captured in a parallel line to the course of the Ammer River

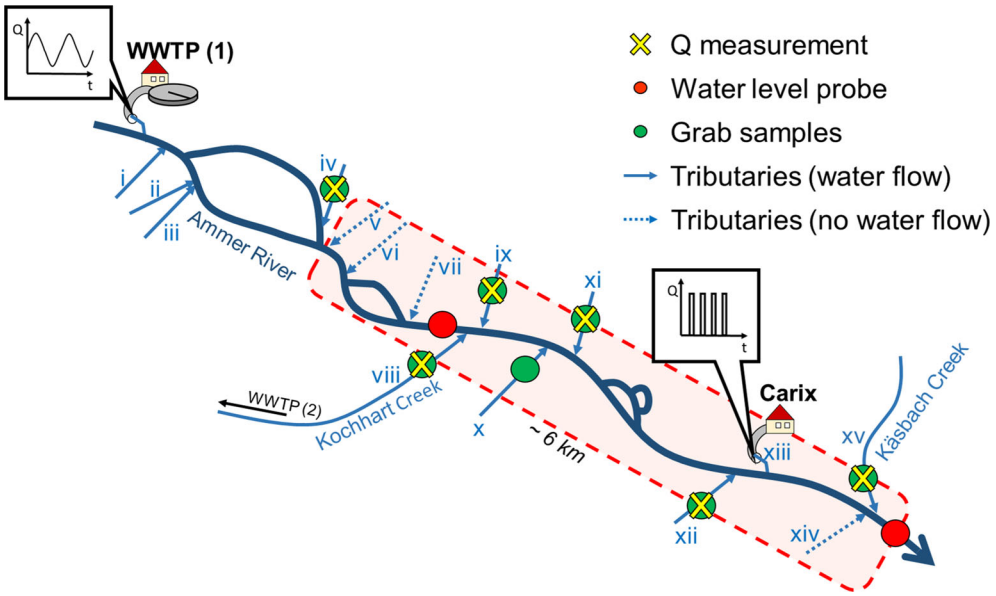

FIGURE 2 Conceptual design of the investigation area downstream of the WWTP 1 with the two main tributaries Kochhart (WWTP 2-influenced) and Käsbach. In addition to samples and manual discharge measurements obtained in the Ammer River (not shown in this graph) long-term rating curve data received from water level probes (red circles) were used for discharge determination. In all tributaries, grab samples for chemical analysis (green circle) and discharge measurements (yellow cross) were conducted. Temporally varying discharge patterns of the wastewater treatment plant (WWTP) and a drinking water treatment plant (Carix) are presented conceptually (inserted speech boxes)

Lischeid, 2013; Ufrecht, 2002), including the Kochhart sub-catchment (Figure1b). Downstream of this, gypsum-rich Middle Keuper formations ('Gipskeuper') overlay the limestone (Villinger, 1982). The Käsbach sub-catchment is characterized by mudstone of the Lower Keuper and overlain by Middle Keuper gypsum formations (http://maps.lgrb-bw.de/) which leads to high sulphate concentrations in this tributary. From a hydrogeological point of view, groundwater flow follows from the recharge areas located west and north of the city of Herrenberg in southeastern direction towards the Neckar River. In this geological context, the studied Ammer segment serves as one main receiving water body with groundwater contours showing a large-scale convergence of groundwater flow towards the Ammer main stem (Ufrecht, 2002, 2006). The Ammer River is therefore unlikely (a) to feature important loosing segments or (b) to be vulnerable to extreme droughts due to the large storage capacity of the contributing karst system. This is expressed by a strong baseflow (Schwientek, Osenbrück, & Fleischer, 2013).

2.2 | Sampling procedure

2.2.1 | General sampling approach and settings

Sampling took place from 19th to 21st of June 2018, during base flow conditions of a, in general, dry summer. Weather conditions were relatively stable (dry and sunny with few clouds). Air temperature according to data provided by the Environmental Agency of the State of Baden-Württemberg ranged from 14.1 to 29.8°C. Water temperature obtained from conductivity temperature depth (CTD) measuring stations ranged from 11.0 to 17.4°C. The distances between the sampling points recorded with a GPS were measured using QGis and cross-checked by measurements in GoogleEarth. All tracers were considered conservative and selected based on the following categorical properties: (a) no expected influence from the WWTP (^{222}Rn); (b) dominant influence from rock dissolution (SO_4^{2-}, EC); (c) affected by geology and land use, but predominantly originating from the WWTP (Cl^-, Na^+); and (d) originating exclusively from the WWTP and generally considered conservative (carbamazepine – CAR, tramadol – TRA).

Two contrasting sampling strategies in the Ammer River were conducted and compared based on the possible influence of the WWTP. The first approach was based on a steady-state assumption for the Ammer River, whereby grab samples for ^{222}Rn, SO_4^{2-}, Na^+, Cl^- and EC measurements were obtained in a **h**igh spatial **r**esolution (HR, 44 samples at 33 sampling locations, distance <300 m between sampling points). The HR sampling took 3 days in total (June 19-21, 2018). The second approach with a focus on the WWTP-associated compounds took the travel time of the water parcels into account ('Lagrangian sampling'; one-day sampling on June 19, 2018). The methodological approach to estimate the travel time of the Ammer River is based on the concept of tracking prominent EC-peaks that originated from the WWTP along the river from EC time series measurements. The EC concentration at a downstream location can be calculated by convoluting the inflowing EC concentration with the transit time distribution function which includes the fitting of the mean travel time and the dispersion parameter. The latter was identified as small and insensitive towards the mean travel time and was therefore not considered for further interpretation, especially with

respect to the potentially larger effect of the measurement uncertainty in comparison to the effect of dispersion. More details of this method are described elsewhere (Glaser et al., 2020). Mean travel time and the respective distance between the sampling sites can be used to compute the arrival time of a certain water parcel at a selected sampling site. This sampling strategy consequently results in a lower number of sampling locations (low spatial resolution, LR) due to logistical reasons. Samples for TRA, CAR, SO_4^{2-}, Cl^- and Na^+ were taken (in total 11 samples, 11 locations) on June 19, 2018. In both cases, sampling took place in flow direction. For the tributaries, steady-state flow conditions were assumed. Lagrangian-sampling (LR) was compared to grab samples (HR). The mass balance-based finite element model FINIFLUX (Frei & Gilfedder, 2015) was used for calculating GW inflow using all selected tracers.

2.2.2 | Chemical sampling and measurements

All SW samples were taken at about 5 cm beneath the water surface in the middle of the river assuming well-mixed conditions at each location which was tested beforehand at two different locations along the river (Figure S2). Grab samples were taken in the tributaries. For ^{222}Rn samples, water was carefully filled into 1 L bottles which were closed tightly without any head space in the bottle until the measurement of the sample. The analysis was conducted shortly after sampling using the portable radon-in-air monitor RAD7 (Durridge Company, Inc.) with the H_2O accessory (Lee & Kim, 2006). After purging, each water sample was degassed for 5 min in a closed loop for at least 30 min. Up to six replicate counting runs led to relative errors of 5–10%. Results were multiplied with an empirical correction factor obtained from the regression between measured activities of 1 L bottles with measured activities of standardized 250 ml reference bottles (previous experiments, data not shown) to account for the lower degassing efficiency of the measured volume (1 L) in comparison to the reference volume of 250 ml. The samples were corrected for radioactive decay between the time of sampling and time of measurement. Ion samples were taken in 100 ml amber glass bottles. EC along with water temperature (WTW ProfiLine Cond 3310, Germany) was measured approximately 5 cm beneath the water surface and temperature-compensated according to Deutsches Institut für Normung (1993).

For organic micropollutant samples, 1 L amber glass bottles were used. Before sampling of ions and organic micropollutants, the bottles were rinsed with sample water. Samples were stored in cool boxes and afterwards in the laboratory at 4°C (dark conditions) until analysis (maximum one day storage for organic micropollutants, maximum about one month storage for ions).

For ^{222}Rn, a distinct difference in concentration between groundwater monitoring wells and spring water was highlighted for rivers in Spain (Barberá & Andreo, 2015) and China (Zhao et al., 2018). Thus, the main strategy for obtaining representative GW samples to determine GW endmember actvities was taking samples from springs that directly discharge to the Ammer River (13 samples, up to 3 replicate sampling to reduce deviation). Since spring water is assumed to be representative for the chemical composition of the groundwater, it is hereafter called groundwater sample (GW). EC values of these springs were used as the first step to distinguish between different geological settings since ion concentrations from Triassic Limestone ('Muschelkalk') and Middle Keuper ('Gipskeuper') groundwater differ significantly. Tracer measurements (^{222}Rn, ions, EC, organic micropollutants) of each geological setting were averaged for a representative GW endmember concentration. The discrete point source 'Schwärzenbrunnen' was treated as an independent endmember since previous investigations identified infiltrating Kochhart Creek water [influenced by WWTP (2)] as origin of this inflow (Harreß, 1973). A volume of 250 ml bottles were used for ^{222}Rn GW samples due to the expected higher activities compared to river water. For ion samples, 100 ml amber glass bottles were used and rinsed with spring water before sampling. Processing after sampling, sample preparation and analysis of major ions are described in more detail in Glaser et al. (2020), organic micropollutant analysis is described in Müller et al. (2018). Ion chromatography (DX 500, DIONEX) was used for the determination of ion concentrations, and organic micropollutants were measured by a tandem mass spectrometry using an *Agilent* 6490 iFunnel Triple Quadrupole (QqQ) instrument (*Agilent Technologies*; see Glaser et al., 2020, for more details). All samples were measured at the Center for Applied Geoscience of the University of Tübingen.

2.2.3 | Measurements of hydrological parameters

In the Ammer River, discharge (*Q*) was determined in at least eightfold replicates in cross profiles per sampling site to minimize measurement uncertainties using the SonTek Acoustic Doppler Current Profiler (ADCP, RiverSurveyor; SonTek, San Diego, USA). In shallow river sections (depth <0.2 m), for which the ADCP is not appropriate, an Acoustic Digital Current meter (ADC; Ott C2, Kempten, Germany) was used for discharge measurements with velocity measurements in at least eight depth profiles (three depths) per cross section. In total, *Q* was measured at 26 locations using the ADCP and at six locations using the ADC along the reach. Additionally, water level time series (time interval 15 min) from two existing measuring stations (OTT CTD, Kempten, Germany) along the river together with appropriate long-term rating curves were used for *Q* determination. *Q* of the two main tributaries Kochhart creek and Käsbach creek were similarly measured using water level time series (time interval 15 min) and pre-existing rating curves. For the additional tributaries (Figure 2), discharge was measured using the ADC as described above for the Ammer main stem (tributaries iv, xi, xii) or estimated by visual judgement (tributaries i-iii, iv,xiii) where flow measurements were not possible due to the shallow water depth. Data evaluation of the ADCP measurements were done using the Matlab based Velocity Mapping Toolbox (Tomas, Hopker, Frigo, & Bleninger, 2016).

2.3 | Model application and mass flux quantification

To estimate the groundwater discharge into the Ammer surface water using ^{222}Rn, the finite elements implicit numerical model FINIFLUX was applied (Frei, Durejka, Le Lay, Thomas, & Gilfedder, 2019). This model was originally set up for ^{222}Rn and based on the following equation:

$$Q\cdot\frac{dc}{dx} = I\cdot(c_{gw}-c) - k\cdot w\cdot c - d\cdot w\cdot\lambda\cdot c + \frac{Q_r}{R_L}(c_{trib}-c) + \frac{\gamma\cdot h\cdot w\cdot\theta}{1+\lambda\cdot t_h} - \frac{\lambda\cdot h\cdot w\cdot\theta}{1+\lambda\cdot t_h}\cdot c \quad (1)$$

where Q [$L^3\ T^{-1}$] is the river discharge, c [$M\ L^{-3}$] is the activity of the tracer and x [L] is the stream length between sampling locations. I [$L^3\ L^{-1}\ T^{-1}$] is the groundwater inflow, c_{gw} [$M\ L^{-3}$] is the concentration in the groundwater, k [$L\ T^{-1}$] is the degassing coefficient, w [L] is the stream width, d [L] the stream depth and λ [T^{-1}] is the decay constant. Q_r [$L^3\ T^{-1}$] is the discharge of the tributaries, R_L [L] the tributary inflow length and c_{trib} [$M\ L^{-3}$] the activity measured in the tributary. θ [–], h [L] and t_h [T] are the hyporheic exchange parameters, namely the porosity of the streambed, the depth of the hyporheic exchange layer, and the mean residence time of water in the hyporheic zone, respectively, and γ [$M\ L^{-3}\ T^{-1}$] is the production rate of ^{222}Rn within the hyporheic zone. For the parameterization of the degassing coefficient, we applied a degassing equation based on Bennett and Rathbun (1972) and Genereux and Hemond (1992). Overall, this mass balance describes the spatial tracer mass flux development along the river ($Q\cdot\frac{dc}{dx}$) as a function of the tracer exchange with the groundwater flux ($I\cdot(c_{gw}-c)$), the sink terms 'degassing' ($k\cdot w\cdot c$) and 'radioactive decay' ($d\cdot w\cdot\lambda\cdot c$), the additional inflow via tributaries ($\frac{Q_r}{R_L}(c_{trib}-c)$) and the source term 'hyporheic exchange' (exponential residence time distribution). The latter may contribute to the tracer mass flux in the river due to the additional production of the tracer ($\frac{\gamma\cdot h\cdot w\cdot\theta}{1+\lambda\cdot t_h}$), or decrease the tracer mass flux ($\frac{\lambda\cdot h\cdot w\cdot\theta}{1+\lambda\cdot t_h}$) in the river due to (radioactive) decay in this zone. For conservative compounds not undergoing decay, degassing or hyporheic enrichment, the mass balance can be simplified as follows:

$$Q\cdot\frac{dc}{dx} = I\cdot(c_{gw}-c) + \frac{Q_r}{R_L}(c_{trib}-c) \quad (2)$$

with the compound concentrations c and c_{gw} [$M\ L^{-3}$; mg L^{-1} for ions, µS cm^{-1} for EC and ng L^{-1} for micropollutants] in the river water, groundwater and tributary, respectively. The model was adapted for conservative compounds in the open source MATLAB code of FINIFLUX (http://www.hydro.uni-bayreuth.de/hydro/en/software/software/software_dl.php?id_obj=129191). Rainfall, evaporation and mixing with stream tributaries were assumed to be negligible for the mass balances during the time of sampling. All concentration measurements are used as model input. Since the number of concentration measurements is higher compared to the measurement points of Q, the latter was linearly interpolated between measurements for missing values for all model setups. Additionally, erroneous values obviously influenced by the discharge pattern of the WWTP or arising from estimations of Q that were uncertain due to the locally large amount of macrophytes in the river channel were removed from the dataset.

3 | RESULTS

3.1 | Environmental boundary conditions and in-stream concentrations of selected compounds

In the Ammer River, measured discharge increased from 0.53 (± 0.05) to 0.78 (± 0.06) $m^3\ s^{-1}$ between the upper and lower ends of the investigation reach. ^{222}Rn activities ranged from 500 to 3,300 Bq m^{-3} (Figure 3a). Similar activities (3000–3,300 Bq m^{-3}) were observed at the first sampling points and between x = 2,340 and 2,620 m downstream of the start of the reach following sharp increases. Three minor, but still significant peaks were observed between 830 and 1,070 m, at 1,650 and 3,200 m along the reach. SO_4^{2-} concentrations ranged from 224 to 291 mg L^{-1} (Figure 3c,h). No significant peaks were detectable. Concentrations were relatively constant along the upper part of the reach at ~280 mg L^{-1}, but decreased rapidly and flattened out to a value of 240 mg L^{-1} at x = 2,500 m. EC ranged from 1,198 to 1,277 µS cm^{-1} (Figure 3b). The spatial development of EC was comparable to SO_4^{2-} concentrations, except for a sharp increase only occurring for the EC at x = 4,310 m. Cl^- and Na^+ ranged from 62 to 72 mg L^{-1} and from 32 to 39 mg L^{-1}, respectively (Figure 3d,e,i,j). Both ion concentrations were similar in their spatial development and strongly correlate (R^2 =.71 for HR, R^2 = .76 for LR). For the HR sampling approach, higher Cl^- and Na^+ concentrations occurred between x = 1,360 and 2,050 m of the reach followed by a decrease in concentrations and afterwards a slight increase down to the section of geological transition (x = 4,840 m). In the segment dominated by Middle Keuper, concentrations decreased again. For the LR sampling approach, the highest concentrations were observed between x = 2,050 and 2,620 m. This pattern partly overlaps with the HR sampling approach. Further downstream (x > 4,200 m), the profiles did not show any other dominating higher concentrations. CAR concentrations ranged from 106 to 161 ng L^{-1}, TRA concentrations ranged from 48 to 73 ng L^{-1} (Figure 3f,g). Two minor peaks were observed at x = 2,250 m and 4,600 m. A strong correlation (R^2 = .91) between CAR and TRA exists (Figure S3).

Groundwater ^{222}Rn endmember activities derived from the spring water samples differ significantly (p < .05, t test) between different geological settings with 19,694 ± 1,998 Bq m^{-3} for Triassic Limestone (n = 6) and 11,500 ± 2,916 Bq m^{-3} for Middle Keuper formations (n = 5). This was also the case for the Triassic Limestone ion concentrations with 91 ± 1 mg L^{-1} for SO_4^{2-}, 33 ± 8 mg L^{-1} for Na^+ and 75 ± 12 mg L^{-1} for Cl^- and EC of 915 ± 82 µS cm^{-1}. For the Middle Keuper formations, SO_4^{2-} and the EC are significantly higher with 1,160 ± 11.6 mg L^{-1} and 2,130 ± 371 µS cm^{-1}, while Na^+ and Cl^- show lower concentrations with 14 ± 1 and 54 ± 4 mg L^{-1}, respectively.

In GW, concentrations of CAR and TRA were below the limit of detection, except for one sample from the tributary ix (Figure 2),

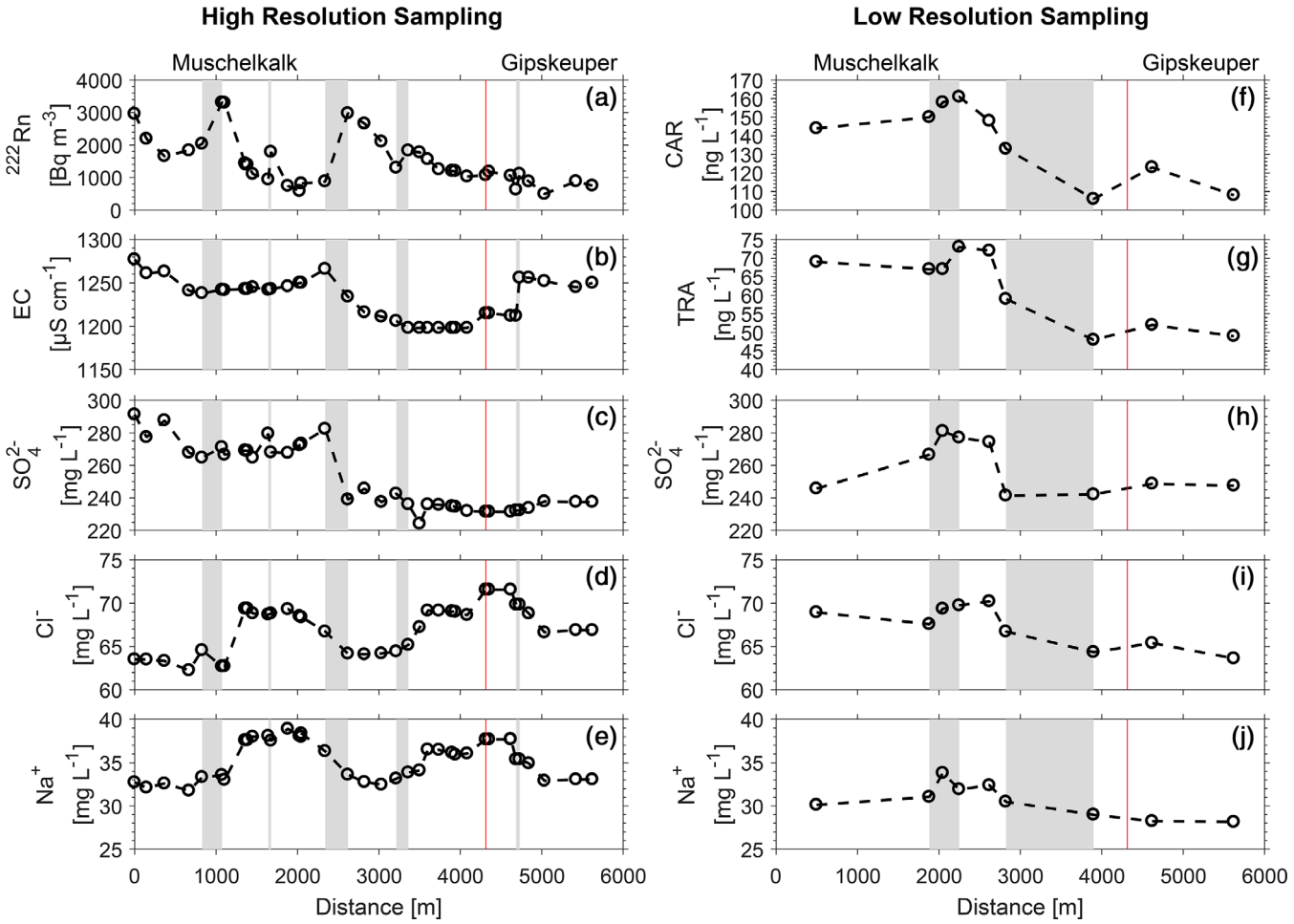

FIGURE 3 Concentrations along the investigation reach starting from the upstream sampling point (0 m). Two different sampling strategies led to different spatial resolutions. Steady-state (3 days of sampling) was assumed for ^{222}Rn (a), EC (b), SO_4^{2-} (c), Cl^- (d), Na^+ (e) and a Lagrangian Sampling approach (1 day of sampling) was applied for carbamazepine (CAR) (f), tramadol (TRA) (g), SO_4^{2-} (h), Cl^- (i), Na^+ (j) leading to less samples along the reach. Grey areas highlight notable changes of ^{222}Rn activities for the high resolution sampling approach and changes of CAR for the low resolution, respectively. The red line indicates the shift from Triassic Limestone ('Muschelkalk') to Middle Keuper ('Gipskeuper') geology

which is spring water contributing to the river. For this tributary, CAR was detected with 54 ng L^{-1} and also the other measured environmental tracer concentrations differed compared to the expected geological signal with 116 mg L^{-1} for SO_4^{2-}, 23 mg L^{-1} for Na^+ and 58 mg L^{-1} for Cl^- and EC of 975 µS cm^{-1} and 10,108 ± Bq m^{-3} for ^{222}Rn which is similar to the Schwärzenbrunnen (tributary x) activity (10,307 Bq m^{-3}). Replicate samples of all measurements to test the temporal variability and thus reliability of the GW samples demonstrate a low standard deviation between samples of the same sampling site (http://hdl.handle.net/10900.1/c6e4a568-1d95-4046-95f9-36bc27202427). In the main tributaries Kochhart and Käsbach, ^{222}Rn activities were relatively low (102–197 Bq m^{-3}). Ion concentrations differed between tributaries (Table 1). CAR and TRA were detectable in the Kochhart creek only.

TABLE 1 Concentrations of investigated compounds (single measurements) in the two main tributaries Kochhart (WWTP 2-influenced) and Käsbach

	Kochhart	Käsbach
^{222}Rn [Bq m^{-3}]	102	197
SO_4^{2-} [mg L^{-1}]	66	247
Cl^- [mg L^{-1}]	116	116
Na^+ [mg L^{-1}]	58	28
EC [µS cm^{-1}]	782	1,250
CAR [ng L^{-1}]	127	<LOD
TRA [ng L^{-1}]	43	<LOD

Abbreviations: EC, electrical conductivity; CAR, carbamazepine; LOD, limit of detection; TRA, tramadol; WWTP, wastewater treatment plant.

3.2 | Estimated groundwater inflow

For all environmental tracers, except for Na^+ and Cl^-, and SO_4^{2-} in the low resolution sampling ($R^2 \leq .28$; Table 2) the coefficient of determination ($R^2 > .88$) showed a good linear fit between modelled values and the measured data. Comparing the normalized standard deviation of the residuals (normalized root mean square error) showed the smallest values for ^{222}Rn (NRMSE = 0.10; Table 2) and thus the smallest deviation from the 1:1 regression between modelled and measured data. This indicates that FINIFLUX applied for ^{222}Rn fits the data well (Figure 4a,b), contrasting to for example, CAR (Figure 4c,d). The modelled ^{222}Rn-based groundwater inflow indicates some high inflow rates up to $4{\cdot}10^{-4}$ m^3 m^{-1} s^{-1} that dominate the overall pattern (Figure 5). EC modelling results agreed with ^{222}Rn-based modelling results in the pattern of GW inflow, but not in the absolute flux of GW volume (maximum $1.3{\cdot}10^{-4}$ m^3 m^{-1} s^{-1}). CAR and TRA inflows follow a similar spatial pattern, and SO_4^{2-} LR shows similar locations of GW exfiltration like ^{222}Rn and EC. Modelled cumulative groundwater inflow using FINIFLUX ranged from 0.022 m^3 s^{-1} (based on Na^+) to 0.265 m^3 s^{-1} (based on ^{222}Rn; Table 2).

4 | DISCUSSION

4.1 | Comparison of selected tracers

4.1.1 | General interpretability of concentration patterns

The dynamics of WWTP effluents significantly influence the selection of an appropriate sampling strategy and thus the general interpretability of selected tracers. For ^{222}Rn activity measurements, no influence of the WWTP can be determined. Reliable replicate measurements at the same location further downstream in the investigation area but at different times of the day under the prevailing conditions during the sampling period are similar (http://hdl.handle.net/10900.1/c6e4a568-1d95-4046-95f9-36bc27202427). These arguments demonstrate that grab samples along the river are representative and thus high ^{222}Rn activities in the river are indicative for GW inflows. The high ^{222}Rn activities in the Ammer River indicate a strong GW-influence, supported by exceptional sharp increases in ^{222}Rn activities along certain reaches of the river (Figure 3a). Classical first order decreases in ^{222}Rn activities such as for the first and third prominent ^{222}Rn peak (grey areas, Figure 3a) mainly arise from radioactive decay and degassing (Cartwright et al., 2011). In general, the observed range of ^{222}Rn activities in the Ammer River is higher compared to previous investigations at different river systems, which were generally between 50 and 1,400 Bq m^{-3} (Atkinson et al., 2015; Mullinger, Binley, Pates, & Crook, 2007; Unland et al., 2013) and can be explained by groundwater that contributes significantly to (perennial) karstic rivers (Bailly-Comte, Borrell-Estupina, Jourde, & Pistre, 2012) compared to many river systems connected to porous aquifers.

The choice of an appropriate sampling strategy could be more relevant for tracers originating from the WWTP. A diurnal cycle of WWTP-derived ions and organic compounds has been described by previous investigations (e.g., Majewsky, Farlin, Bayerle, & Gallé, 2013; Salgado et al., 2011; Schwientek et al., 2016). Comparing Cl^- and Na^+ concentrations of the sampling approach by (a) assuming steady state (HR) and (b) taking travel time of the water parcels into account (LR) demonstrates a significant difference in ion concentrations along the selected river segment (Figure 3d,e,i,j). Even if the first peak of high concentrations at a distance of ~2,000 m downstream of the most upstream sampling point is detectable for both sampling strategies, a second very broad peak (between ~3,500 and 4,500 m) can only be seen for the HR sampling approach for both ions (Figure 3d,e). Previous research demonstrated that an appropriate sampling approach (Lagrangain sampling) that considers the dynamics of the WWTP is required for comparisons of water samples taken along a river profile when aiming to describe the fate of organic micropollutants (e.g., Antweiler, Writer, & Murphy, 2014; Kunkel & Radke, 2012; Writer, Antweiler, Ferrer, Ryan, & Thurman, 2013). Therefore, we suggest that concentration patterns of Na^+ and Cl^- (HR) reflect 'wastewater waves' in the river water during the time of the sampling (3 days). High ion concentrations of HR can, therefore, indicate high WWTP discharge conditions rather than locations of GW inflow. Neglecting the influence of dynamic WWTP releases of these tracers, which in our case corresponds to the HR scenario, leads to a wrong interpretation of the groundwater inflow using Na^+ and Cl^- as tracers.

TABLE 2 Regression coefficients (R^2) and NRMSE (normalized root mean square error, normalized to the difference between the maximum and minimum value of the respective dataset) between measured and modelled activity, electrical conductivity and concentrations, respectively, and cumulative GW inflow along the tested river reach, based on modelling results with FINIFLUX for the high resolution (HR) and low resolution (LR) sampling approach

		R^2	NRMSE	Cumulative GW inflow [m^3 s^{-1}]
HR	^{222}Rn [Bq m^{-3}]	.92	0.10	0.265
	EC [µS cm^{-1}]	.88	0.41	0.082
	SO_4^{2-} [mg L^{-1}]	.88	0.49	0.059
	Cl^- [mg L^{-1}]	.04	0.49	0.043
	Na^+ [mg L^{-1}]	.11	0.54	0.050
LR	CAR [ng L^{-1}]	.93	0.26	0.091
	TRA [ng L^{-1}]	.88	0.27	0.112
	SO_4^{2-} [mg L^{-1}]	.28	0.41	0.059
	Cl^- [mg L^{-1}]	<.01	0.44	0.026
	Na^+ [mg L^{-1}]	.02	0.37	0.022

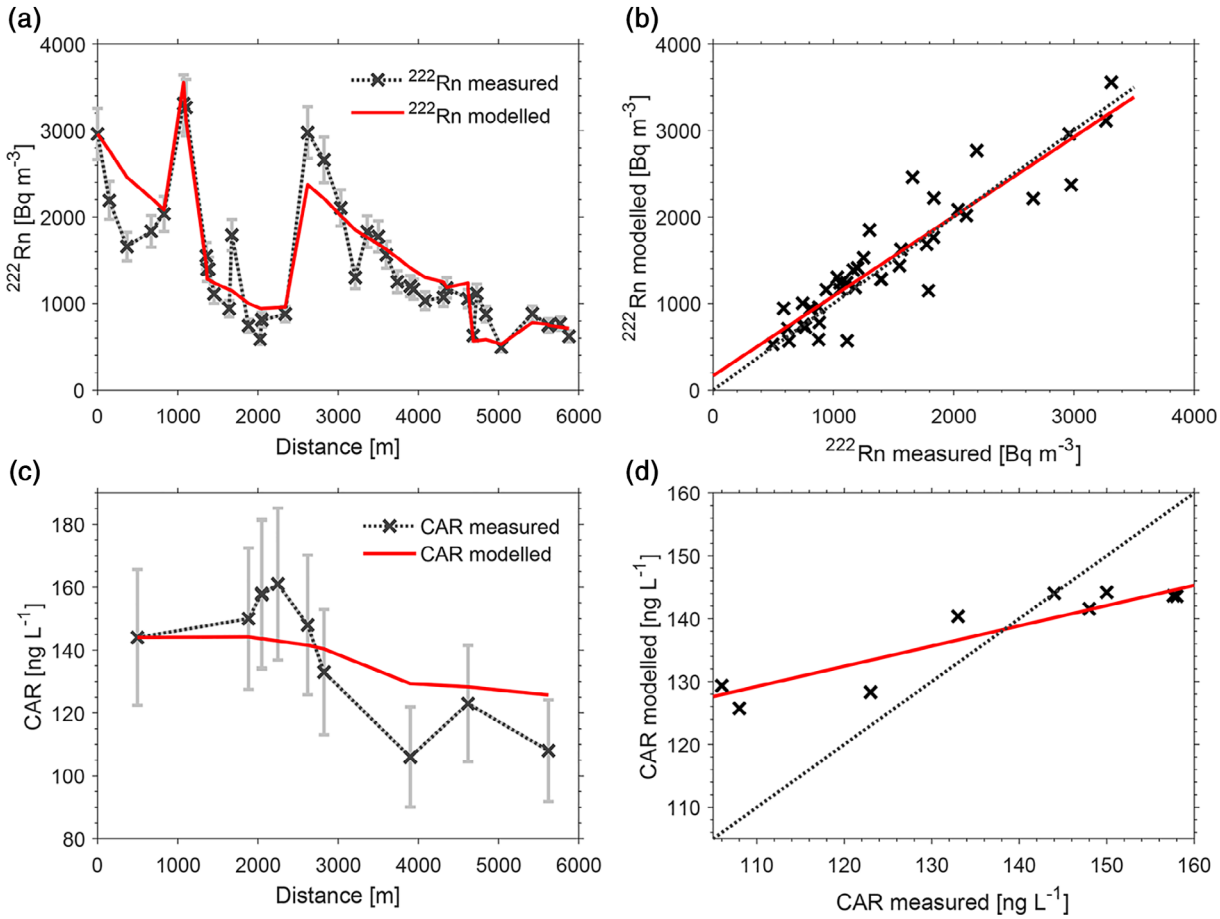

FIGURE 4 Measured and modelled (a) ^{222}Rn activity with measurement uncertainty (grey errorbars, 10%) and (c) carbamazepine (CAR) concentrations with measurement uncertainty (grey errorbars, 15%) of the investigation reach starting from the upstream sampling point (0 m) and corresponding agreement of measured and modelled (b) activity and (d) concentrations, respectively. The dotted lines in (b) and (d) indicate a 1:1 agreement, the red lines in (b) and (d) result from linear regressions of modelled versus measured activities/concentrations

Comparing SO_4^{2-} concentrations of the HR sampling strategy with Na^+ and Cl^- (HR) does not show the 'wastewater waves' as described for Na^+ and Cl^-. However, SO_4^{2-} HR results differ strongly from the LR sampling approach, especially in the upstream segment. High SO_4^{2-} concentrations (HR) occur at the same time as low concentrations of Na^+ and Cl^- (HR) in the river (Figure 3), which is obviously due to low WWTP discharge conditions. Low WWTP effluent discharge might lead to a high SO_4^{2-} signal, arising from the gypsum-bearing geology located between the WWTP and the most upstream sampling location. This indicates that SO_4^{2-} is in general a more suitable tracer compared to Cl^- and Na^+ though still influenced by the WWTP. EC (HR) as a sum parameter representing the ion concentration of the river is similar to the SO_4^{2-}-concentrations along the reach (Figure 3), except for the very prominent EC increase at 4,700 m from the most upstream sampling point. This very steep increase can most likely be attributed to wrong measurement settings of the device, since none of the ion concentrations follows this pattern.

4.1.2 | Applicability of tracers for GW quantification

A quantitative interpretation of tracer concentrations with regards to GW exfiltration is uncertain due to different GW endmember concentrations arising from different geological settings (Figure 3). Thus, applying FINIFLUX for better comparability between tracers may be a suitable evaluation method for the quantification of GW inflows. 'Traditional' approaches linearize the first-order derivative in the ordinary differential equation, followed by solving the mass balances for groundwater inflows into rivers ('inversion'; e.g., Mullinger et al., 2007; Unland et al., 2013). This may lead to physically implausible negative fluxes or instabilities hidden within positive results that look realistic, especially for large spatial scale data. FINIFLUX accounts for these numerical instabilities by discretizing the ODE under application of a parameter optimization approach ('finite element model'; Frei & Gilfedder, 2015). However, modelling results of FINIFLUX based on different tracers strongly differ in the estimated amounts of

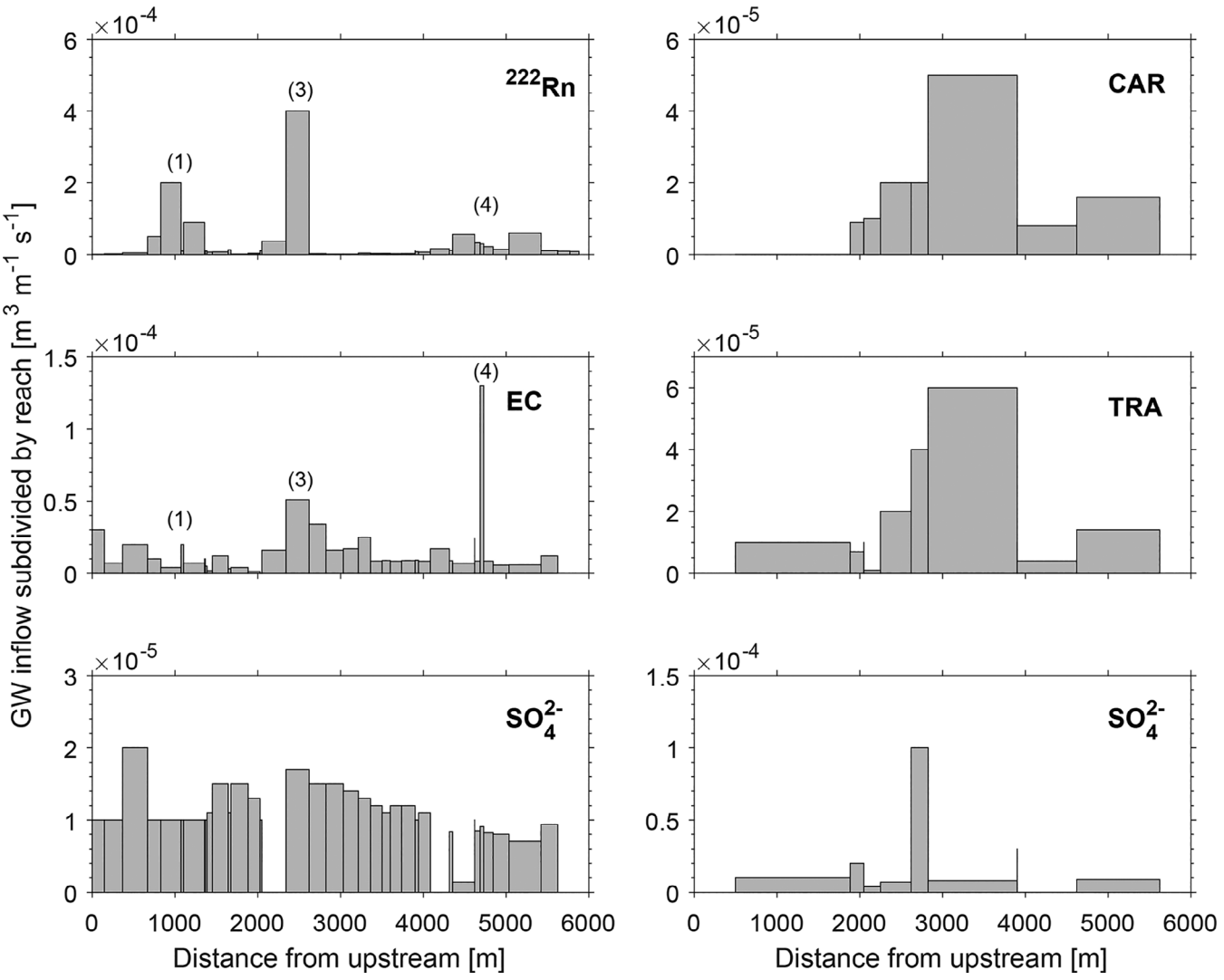

FIGURE 5 Modelled groundwater inflow using the model FINIFLUX based on the tracers radon (^{222}Rn), carbamazepine (CAR), electrical conductivity (EC), tramadol (TRA) and sulphate (SO_4^{2-}) with two different sampling settings [left: spatially high resolution (HR), right: spatially low resolution (LR)]

water and in the GW exfiltration locations despite partly acceptable coefficient of determination ($R^2 > .88$). The normalized root mean square error (NRMSE) is a complementary parameter to evaluate the goodness of the model fit to measured data and to interpret the modelling results. A high coefficient of determination coupled with a low NRMSE shows the best agreement of modelled and measured data (Figure 4a,b, Table 2). Among the selected tracers, only ^{222}Rn-based modelling leads to realistic results in this modelling case, indicated by the lowest NRMSE (0.10) combined with a high coefficient of determination ($R^2 = 92$) and a plausible water balance. Therefore, FINFILUX seems most applicable for ^{222}Rn in the Ammer catchment and may be reliable for GW inflow localization. This is supported by the fact that the amount of cumulative GW flux (0.265 $m^3\ s^{-1}$, Table 2) is similar compared to the discharge difference between upstream (0.53 ± 0.05 $m^3\ s^{-1}$) and downstream (0.78 ± 0.06 $m^3\ s^{-1}$) location minus the tributary inflow (0.03 ± 0.008 $m^3\ s^{-1}$) and to previous assessments of groundwater inflows ranging between 0.2 and 0.3 $m^3\ s^{-1}$ (Harreß, 1973). This outcome is different compared to all the other environmental tracers, where the modelled groundwater inflow significantly underestimates the discharge difference. However, this amount must be interpreted carefully and should not be the only argument in terms of transferability of this method to other river settings. Underlying assumptions for the determination of ^{222}Rn activity in groundwater is that springs, where samples for the determination of GW endmember activity were obtained from, are representative for the entire reach. In karst environment where degassing in the underground may be relevant, a constantly wrong GW endmember determination would not necessarily affect the calculated pattern of GW exfiltration, but the absolute contribution. Additionally, a potentially smaller 'real' degassing in the river as assumed for this setting could also entail higher GW endmember activities. In rivers embedded in porous media, an appropriate applicability of FINIFLUX for ^{222}Rn was already shown in two former investigations at the rivers Roter Main and Salzach and gives plausible

groundwater fluxes (Frei & Gilfedder, 2015; Pittroff, Frei, & Gilfedder, 2017). In contrast to the previous applications, which covered scales of 32 and 52 km, respectively, the spatial resolution of the study at the Ammer River is higher and thus provides a more detailed insight into the specific localization of the GW inflow. This higher resolution enables detection of steep increases and decreases of ^{222}Rn activities in the Ammer River as described above. This may be the reason of poorer regression coefficients compared to the study results on Roter Main and Salzach (regression coefficients of .99 and .97, respectively) and thus for the slight overestimation of the cumulative GW inflow considering Q increase with associated measurement errors in the investigation area (http://hdl.handle.net/10900.1/c6e4a568-1d95-4046-95f9-36bc27202427).

Only LR-ion modelling results are presented due to the ion HR-setup clearly influenced by the transient ion concentrations, except for SO_4^{2-} which showed acceptable results based on the concentration pattern. Even if measured concentrations from the Lagrangian sampling approach seem more reasonable than from grab sampling, modelling of the ion concentrations (LR) did not show GW inflows in a range similar to ^{222}Rn modelling results or the water mass balance. This may be due to a smaller difference between concentrations in GW and SW for the selected ions, since a difference with a magnitude smaller than a factor of 2 makes ions less sensitive for changes due to GW inflow compared to ^{222}Rn (Gilfedder et al., 2015). Only concentrations of TRA, CAR and SO_4^{2-} differ by a factor of 5 between GW and SW, in case of SO_4^{2-} only for GW from Gypsum Karst. Thus, insensitive modelling may arise from an insufficient end-member determination. This is also the case for EC measurements (HR). For EC, an oversaturation with respect to calcite could occur if saturated groundwater enters (warmer) surface water leading to a degassing of CO_2. This can influence the conservativeness of this tracer and thus restrict its applicability regarding the modelling of GW inflows in karstic environments. Even if the modelled fluxes for ^{222}Rn and EC results are not similar in regard of the absolute volume flux of groundwater, the spatial pattern of GW inflow is similar. This shows that the general geological shift and the resulting difference in endmember EC is appropriate but not sufficient to quantify reliable GW fluxes based on EC measurements.

The influence of an inappropriate GW endmember concentration determination is also illustrated by comparing measured and modelled data of ^{222}Rn with CAR (Figure 4). For conservative compounds such as CAR, high measured concentrations are underestimated by the modelled values and reverse for small measured values (Figure 4c,d). The first aspect might be explained by an underestimated GW endmember concentration or due to unexpected contaminated GW inflow into the river (further discussed below). Overestimated modelled values for low concentrations may be ascribed to potentially implausible model assumptions for this compound such as the absence of a degradation term for CAR. Although a small attenuation potential is typically ascribed to this compound (half-life of 50 hr for the Ammer River, Glaser et al., 2020), even a slow degradation might be still relevant in terms of GW exfiltration modelling similar to the comparably small radioactive decay in case of ^{222}Rn ($t_{0.5}$ = 3.8 days). Additionally, the concentration range of CAR is considerably smaller compared to the range of ^{222}Rn activity impeding interpretation, and the analytical measurement error (~15%) comes more into effect for the overall small CAR concentrations. This uncertainty propagates through the modelling results. Nevertheless, NRMSE of organic micropollutants are second lowest following ^{222}Rn results indicating that these compounds might be applicable for river systems with no prevailing concentrations in groundwater and by including a compound specific sink term. Further investigations and a larger data set of CAR in the respective investigation are necessary for validation under different hydrological conditions.

4.2 | Localization of GW inflow – conceptual model for the investigation area

Based on a combination of the tracer results as described in the following, a conceptual model was developed for groundwater inflow including stream network patterns and proposed groundwater flow (Figure 6). This conceptual model can reasonably explain the observations along the reach. The most remarkable concentration change for nearly all tracers in SW is between 2,340 and 2,620 m and leads to the highest GW inflow based on the ^{222}Rn-modelling results. This GW inflow may be attributed to the Schwärzenbrunnen, a known and extended groundwater exfiltration zone on the right bank of the Ammer River extending over a distance of about 10 m and dominating the GW inflow of the whole investigation area (~50% of overall GW inflow). Besides this important inflow, further sharp ^{222}Rn increases indicate that discrete GW inflows prevail along the study segment. Bailly-Comte et al. (2009) suggest that concepts for porous media aquifers may be applicable for karst aquifer-surface water interaction, even though they also identified a SW–GW interaction controlled by prevailing fractures and conduits (Coulazou River, Southern France). In contrary, our results are in accordance with other karst rivers, where GW discharge occurs primarily at discrete point sources because of open fractures (Oxtobee & Novakowski, 2002).

The locations of ^{222}Rn activitiy increases and modelled GW inflow can be attributed to the geological setting of the study area. Previous studies in the Ammer catchment attribute a favoured karstification by the degassing of CO_2 along faults (Harreß, 1973) which may arise from lithological deeper layers. Further investigations confirmed faults by soil CO_2 mapping profiles and postulate faults in a pronounced orientation in WSW-ENE direction within the catchment from an implicit geological modelling approach (D'Affonseca, Finkel, & Cirpka, 2020). The stream network in the Ammer catchment largely follows this orientation. If straight segments of tributary valleys are extended, they intersect the Ammer River at locations with changes in selected measured environmental tracers in the river water and resulting calculated GW inflows (Figure 6). The attribution of GW inflow to small-scale, so far unmapped faults in the catchment is in accordance with previous interpretations of the geological settings in southwestern Germany. Ufrecht (2006) already claimed that small-scale geological fractures may exist that are not captured by

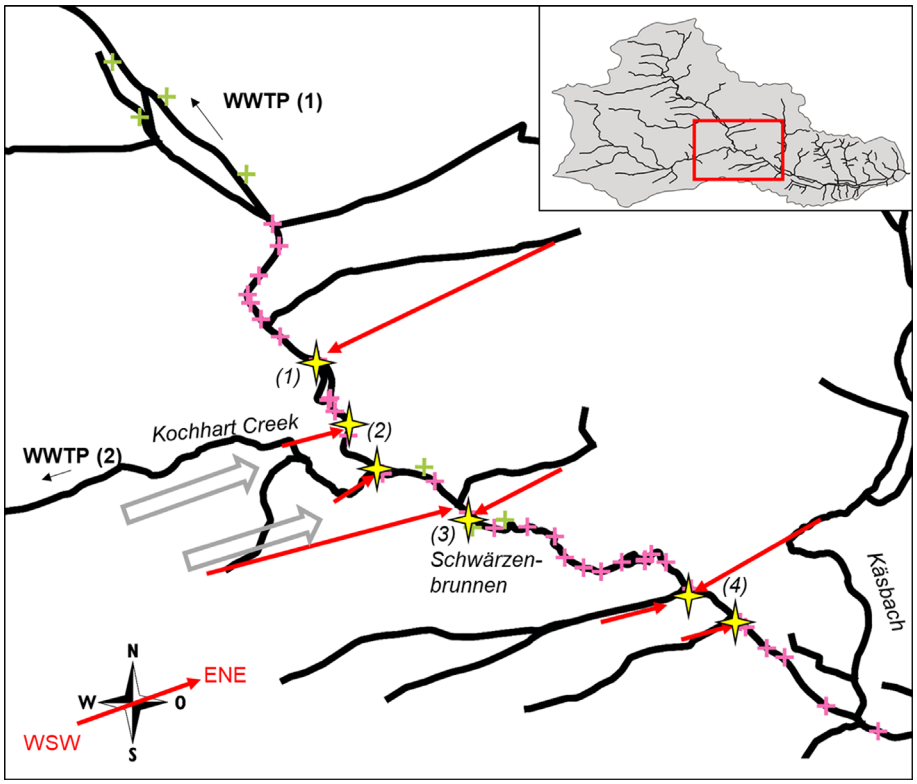

FIGURE 6 Conceptual model of groundwater flow into the investigation reach. Straight stream segments were extended in WSW-ENE direction (red arrows) according to the orientation of the dominating faults in the catchments. Extensions meet sampling locations [(1),(2),(3),(4)] with changes in concentrations of environmental tracers (^{222}Rn, SO_4^{2-}). Grey arrows indicate proposed origins of the GW from infiltrated Kochhart water (that contains organic micropollutants from the wastewater treatment plant). The pinkish crosses indicate the sampling sites in the surface water, while the green crosses highlight the groundwater sampling sites

geological maps, but may though be relevant for the groundwater flow. Former investigations hypothesized that the general pattern and structure of a river network can indicate underlying structures, and the chronology of geological events, which could influence GW-SW connection (Raj, 2007; Twidale, 2004). A case study in a karstified catchment (Spain) demonstrated a correspondence between the fault direction and orientation of stream channels (Gelabert, Fornós, Pardo, Rosselló, & Segura, 2005). In karstic systems, geological faults may lead to a self-reinforcing process by which enhanced GW flow along faults accelerates the karstification and, in turn, further increases the water flow. Thus, in the development of karst conduits and exfiltration into rivers may be largely governed by the orientation and location of faults and fissures. For the areas with a large number of faults, a change in ion concentrations can be seen for LR samples, even if a comparison is restricted due to the lower resolution.

Increased concentrations of CAR are in accordance with some of the earlier described locations of preferential GW inflow due to geological settings which are located, in detail, where straight segments of the Kochhart creek and the Schwärzenbrunnen are extended to the Ammer River (Figure 6 (2) and (3)). This indicates that the assumption of no prevailing organic micropollutant concentrations in the GW may not be valid for the Ammer catchment. In addition, the measurement uncertainty of the organic compounds can highly impact the wrong assumption of no prevailing micropollutants. It thus explains the unreliable modelled GW fluxes based on CAR data due to an underestimation of CAR endmember concentrations (Figure 4d). For a karstic catchment in the United Kingdom, organic micropollutants have been described to occur in groundwater and enter SW where the gradient is from the aquifer to the SW (Manamsa et al., 2016). Increased concentrations in the river water may point out the origin of the GW. It has been established in previous studies that water of the Kochhart creek downstream of the WWTP (2) (Figure 1) infiltrates into the GW (Harreß, 1973). At the same time, other organic micropollutants, apart from TRA and CAR, have been detected in *tributary* ix and in the Schwärzenbrunnen (http://hdl.handle.net/10900.1/c6e4a568-1d95-4046-95f9-36bc27202427). These organic micropollutants could originate from WWTP (2) and support the previously described hydraulic connection between the Kochhart creek and the Schwärzenbrunnen (Harreß, 1973). Lower concentrations in the Schwärzenbrunnen may be explained by the dilution effect of the Kochhart water infiltrating into the GW. The fact that the Schwärzenbrunnen is bearing Kochhart water is supported by the interpreted subsurface water flow direction obtained from previous tracer experiments and water level measurements in the Ammer catchment. These previous findings indicated an easterly subsurface water flow direction in the area based on previous tracer tests (D'Affonseca et al., 2020, and references therein). Thus, the GW entering the Ammer segment between Kochhart and Schwärzenbrunnen may, at least partly, originate from the Kochhart creek which may also influence other tracer concentrations.

5 | CONCLUSIONS

This study demonstrates that ^{222}Rn can be used for quantification and localization of GW and is deemed to perform in a more reliable way in

comparison to the other environmental tracers. Concepts describing GW–SW interactions for porous media are hardly transferable to karstic rivers, although, in the studied case, the karstic environment turned out to be a smaller challenge than the transient artificial inputs. Modelled GW inflow based on ^{222}Rn reflects the water budget in the catchment, while other tracers' modelling results significantly underestimate the inflowing GW volume. This is mainly due to a very high concentration difference between GW and SW and the insensitivity of ^{222}Rn towards the influence of the WWTP. However, various (tracer-specific) uncertainties may lead to limited applicability of tracers for groundwater inflow determination. Heterogeneity of (geogenic) GW endmember concentrations restricts GW quantification. For ^{222}Rn, degassing constitutes a source of uncertainty in its application as a groundwater tracer. This is especially relevant if degassing is not captured by for example, gas tracer tests in parallel to the ^{222}Rn measurements. Thus, it is necessary to rely on established degassing equations, which might not represent the particular conditions of the selected system to its full extent. In addition, uncontrollable degassing in the karstified underground before determining a representative endmember activity can cause uncertainties in the application as a groundwater tracer in karstic catchments. For all tracers that (partly) originate from the WWTP, unsteady concentrations caused by the WWTP dynamics lead to uncertainties which is unlikely to be compensated with a higher resolution sampling approach. A steady-state assumption is therefore not appropriate for tracers clearly influenced by the WWTP. Additionally, an erroneous estimation of GW endmember concentrations/activity, not completely mixed water from different origins (e.g., GW–SW, tributary-river) and additional unknown inputs of tracers are important sources of uncertainty. This seems particularly relevant for organic micropollutants in the prevailing karstic river system with partly unexpected contaminated groundwater, but may be of minor importance for other geological settings. Dispersion is a parameter not discussed in detail in this study as well as the accuracy of tracking the same water parcels, but which could be crucial for the mixing between adjoining water parcels for WWTP compounds with comparably small concentrations. Additionally, hydrological turnover measurements (ascertained by artificial tracer tests) that describe the simultaneously occurring water loss and gain at rivers are beyond the scope of this article and were not considered for the data interpretation. However, this aspect might play a role and cannot be excluded from the discharge increase along a river stretch. Despite the fact that many organic micropollutants raise considerable toxicological concern, they are globally omnipresent in aquatic systems and should therefore be considered as 'emerging hydrological tracers' in future studies of hydrological systems various in size and flow.

ACKNOWLEDGEMENTS

This work was supported by the Collaborative Research Center 1253 CAMPOS (Project P1: Rivers) funded by the German Research Foundation (DFG, Grant Agreement SFB 1253/1 2017). The authors also acknowledge financial support by the Excellence Initiative at the University of Tübingen, funded by the German Federal Ministry of Education and Research and the German Research Foundation (DFG). The authors thank Bernhard Sulger, Dakota Tallman, Eva Voggenreiter, Oliver Nied, Stephanie Nowak, Sara Cafisso and Bernice Nisch for support in sampling and assisting in the laboratory and Karsten Osenbrück for providing the geological profile.

DATA AVAILABILITY STATEMENT

The data that support the findings of this study are openly available in the data repository "Forschungsdatenarchiv (FDAT)" of the University of Tübingen at http://hdl.handle.net/10900.1/c6e4a568-1d95-4046-95f9-36bc27202427.

ORCID

Clarissa Glaser https://orcid.org/0000-0002-2932-6202

REFERENCES

Antweiler, R. C., Writer, J. H., & Murphy, S. F. (2014). Evaluation of wastewater contaminant transport in surface waters using verified Lagrangian sampling. *Science of the Total Environment*, *470-471*, 551–558.

Atkinson, A. P., Cartwright, I., Gilfedder, B. S., Hofmann, H., Unland, N. P., Cendón, D. I., & Chisari, R. (2015). A multi-tracer approach to quantifying groundwater inflows to an upland river; assessing the influence of variable groundwater chemistry. *Hydrological Processes*, *29*(1), 1–12.

Avery, E., Bibby, R., Visser, A., Esser, B., & Moran, J. (2018). Quantification of groundwater discharge in a subalpine stream using radon-222. *Water*, *10*(2), 100.

Bailly-Comte, V., Borrell-Estupina, V., Jourde, H., & Pistre, S. (2012). A conceptual semidistributed model of the Coulazou River as a tool for assessing surface water-karst groundwater interactions during flood in Mediterranean ephemeral rivers. *Water Resources Research*, *48*, 14.

Bailly-Comte, V., Jourde, H., & Pistre, S. (2009). Conceptualization and classification of groundwater–surface water hydrodynamic interactions in karst watersheds. Case of the karst watershed of the Coulazou River (Southern France). *Journal of Hydrology*, *376*(3–4), 456–462.

Banzhaf, S., Krein, A., & Scheytt, T. (2012). Using selected pharmaceutical compounds as indicators for surface water and groundwater interaction in the hyporheic zone of a low permeability riverbank. *Hydrological Processes*, *27*, 2892–2902.

Barberá, J. A., & Andreo, B. (2015). Hydrogeological processes in a fluviokarstic area inferred from the analysis of natural hydrogeochemical tracers. The case study of eastern Serranía de Ronda (S Spain). *Journal of Hydrology*, *523*, 500–514.

Barberá, J. A., & Andreo, B. (2017). River-spring connectivity and hydrogeochemical interactions in a shallow fractured rock formation. The case study of Fuensanta river valley (Southern Spain). *Journal of Hydrology*, *547*, 253–268.

Bennett, J. P., & Rathbun, R. E. (1972). Reaeration in open-channel flow. *U. S. Geological Survey Professional Paper*, *737*, 75.

Bittner, D., Narany, T. S., Kohl, B., Disse, M., & Chiogna, G. (2018). Modeling the hydrological impact of land use change in a dolomite-dominated karst system. *Journal of Hydrology*, *567*, 267–279.

Brunke, M., & Gonser, T. (1997). The ecological significance of exchange processes between rivers and groundwater. *Freshwater Biology*, *37*(1), 1–33.

Cartwright, I., & Gilfedder, B. S. (2015). Mapping and quantifying groundwater inflows to Deep Creek (Maribyrnong catchment, SE Australia) using ^{222}Rn, implications for protecting groundwater-dependant ecosystems. *Applied Geochemistry*, *52*, 118–129.

Cartwright, I., Hofmann, H., Sirianos, M. A., Weaver, T. R., & Simmons, C. T. (2011). Geochemical and ^{222}Rn constraints on baseflow to the Murray River, Australia, and timescales for the decay of

low-salinity groundwater lenses. *Journal of Hydrology*, *405*(3–4), 333–343.

Clara, M., Strenn, B., & Kreuzinger, N. (2004). Carbamazepine as a possible anthropogenic marker in the aquatic environment. Investigations on the behaviour of carbamazepine in wastewater treatment and during groundwater infiltration. *Water Research*, *38*(4), 947–954.

Cook, P. G. (2013). Estimating groundwater discharge to rivers from river chemistry surveys. *Hydrological Processes*, *27*(25), 3694–3707.

Cook, P. G., Rodellas, V., & Stieglitz, T. C. (2018). Quantifying surface water, porewater, and groundwater interactions using tracers. Tracer fluxes, water fluxes, and end-member concentrations. *Water Resources Research*, *54*(3), 2452–2465.

D'Affonseca, F. M., Finkel, M., & Cirpka, O. A. (2020). Combining implicit geological modelling, field surveys, and hydrogeological modelling to describe groundwater flow in a karst aquifer. *Hydrogeology Journal*.

Deutsches Institut für Normung. (1993). Water quality; Determination of electrical conductivity (ISO 7888: 1985); German Version EN 27888.

Dvory, N. Z., Livshitz, Y., Kuznetsov, M., Adar, E., Gasser, G., Pankratov, I., … Yakirevich, A. (2018). Caffeine vs. carbamazepine as indicators of wastewater pollution in a karst aquifer. *Hydrology and Earth System Sciences*, *22*, 6371–6381.

Frei, S., Durejka, S., Le Lay, H., Thomas, Z., & Gilfedder, B. S. (2019). Quantification of hyporheic nitrate removal at the reach scale. Exposure times versus residence times. *Water Resources Research*, *55*(11), 9808–9825.

Frei, S., & Gilfedder, B. S. (2015). FINIFLUX. An implicit finite element model for quantification of groundwater fluxes and hyporheic exchange in streams and rivers using radon. *Water Resources. Research*, *51*(8), 6776–6786.

Fryar, A. E., Wallin, E. J., & Brown, D. L. (2000). Spatial and temporal variability in seepage between a contaminated aquifer and tributaries to the Ohio River. *Groundwater Monitoring & Remediation*, *20*(3), 129–146.

Gelabert, B., Fornós, J. J., Pardo, J. E., Rosselló, V. M., & Segura, F. (2005). Structurally controlled drainage basin development in the south of Menorca (Western Mediterranean, Spain). *Geomorphology*, *65*(1–2), 139–155.

Genereux, D. P., & Hemond, H. F. (1992). Determination of gas exchange rate constants for a small stream on Walker Branch Watershed, Tennessee. *Water Resources Research*, *28*(9), 2365–2374.

Gilfedder, B. S., Frei, S., Hofmann, H., & Cartwright, I. (2015). Groundwater discharge to wetlands driven by storm and flood events. Quantification using continuous Radon-222 and electrical conductivity measurements and dynamic mass-balance modelling. *Geochimica et Cosmochimica Acta*, *165*, 161–177.

Glaser, C., Zarfl, C., Werneburg, M., Böckmann, M., Zwiener, C., & Schwientek, M. (2020). Temporal and spatial variable in-stream attenuation of selected pharmaceuticals. *Science of the Total Environment*, *741*, 139514.

Gros, M., Petrović, M., & Barceló, D. (2007). Wastewater Treatment Plants as a pathway for aquatic contamination by pharmaceuticals in the Ebro River Basin (Northeast Spain). *Environmental Toxicology and Chemistry*, *26*(8), 1553–1562.

Guillet, G., Knapp, J. L. A., Merel, S., Cirpka, O. A., Grathwohl, P., Zwiener, C., & Schwientek, M. (2019). Fate of wastewater contaminants in rivers. Using conservative-tracer based transfer functions to assess reactive transport. *Science of the Total Environment*, *656*, 1250–1260.

Harreß H. M. (1973). *Hydrogeologische Untersuchungen im Oberen Gäu* (Dissertation). Universität Tübingen.

Harrington, G. A., Gardner, W. P., & Munday, T. J. (2014). Tracking groundwater discharge to a large river using tracers and geophysics. *Groundwater*, *52*(6), 837–852.

Hartmann, A., & Baker, A. (2017). Modelling karst vadose zone hydrology and its relevance for paleoclimate reconstruction. *Earth-Science Reviews*, *172*, 178–192.

Kalbus, E., Reinstorf, F., & Schirmer, M. (2006). Measuring methods for groundwater-surface water interactions: A review. *Hydrology and Earth System Science*, *10*, 873–887.

Kumar, M., Ramanathan, A., & Keshari, A. K. (2009). Understanding the extent of interactions between groundwater and surface water through major ion chemistry and multivariate statistical techniques. *Hydrolocial Processes*, *23*(2), 297–310.

Kunkel, U., & Radke, M. (2012). Fate of pharmaceuticals in rivers. Deriving a benchmark dataset at favorable attenuation conditions. *Water Research*, *46*(17), 5551–5565.

Lee, D. R. (1977). A device for measuring seepage flux in lakes and estuaries. *Limnology and Oceanography*, *22*(1), 140–147.

Lee, J.-M., & Kim, G. (2006). A simple and rapid method for analyzing radon in coastal and ground waters using a radon-in-air monitor. *Journal of Environmental Radioactivity*, *89*(3), 219–228.

Li, Z., Sobek, A., & Radke, M. (2016). Fate of pharmaceuticals and their transformation products in four small European rivers receiving treated wastewater. *Environmental Science & Technology*, *50*(11), 5614–5621.

Majewsky, M., Farlin, J., Bayerle, M., & Gallé, T. (2013). A case-study on the accuracy of mass balances for xenobiotics in full-scale wastewater treatment plants. *Environmental Sciences: Processes & Impacts*, *15*(4), 730–738.

Malaj, E., Ohe, P. C., von, d., Grote, M., Kühne, R., Mondy, C. P., … Schäfer, R. B. (2014). Organic chemicals jeopardize the health of freshwater ecosystems on the continental scale. *Proceedings of the National Academy of Sciences of the United States of America*, *111*(26), 9549–9554.

Manamsa, K., Lapworth, D. J., & Stuart, M. E. (2016). Temporal variability of microorganic contaminants in lowland chalk catchments. New insights into contaminant sources and hydrological processes. *Science of the Total Environment*, *568*, 566–577.

Müller, M. E., Escher, B. I., Schwientek, M., Werneburg, M., Zarfl, C., & Zwiener, C. (2018). Combining in vitro reporter gene bioassays with chemical analysis to assess changes in the water quality along the Ammer River, Southwestern Germany. *Environmental Sciences Europe*, *30*, 20.

Mullinger, N. J., Binley, A. M., Pates, J. M., & Crook, N. P. (2007). Radon in Chalk streams. Spatial and temporal variation of groundwater sources in the Pang and Lambourn catchments, UK. *Journal of Hydrology*, *339*(3–4), 172–182.

Oxtobee, J. P. A., & Novakowski, K. (2002). A field investigation of groundwater/surface water interaction in a fractured bedrock environment. *Journal of Hydrology*, *269*(3–4), 169–193.

Pal, A., Gin, K. Y.-H., Lin, A. Y.-C., & Reinhard, M. (2010). Impacts of emerging organic contaminants on freshwater resources. Review of recent occurrences, sources, fate and effects. *Science of the Total Environment*, *408*(24), 6062–6069.

Payn, R. A., Gooseff, M. N., McGlynn, B. L., Bencala, K. E., & Wondzell, S. M. (2009). Channel water balance and exchange with subsurface flow along a mountain headwater stream in Montana, United States. *Water Resources Research*, *45*, 14.

Pittroff, M., Frei, S., & Gilfedder, B. S. (2017). Quantifying nitrate and oxygen reduction rates in the hyporheic zone using ^{222}Rn to upscale biogeochemical turnover in rivers. *Water Resources Research*, *53*(1), 563–579.

Raj, R. (2007). Strike slip faulting inferred from offsetting of drainages. Lower Narmada Basin, western India. *Journal of Earth System Science*, *116*(5), 413–421.

Salgado, R., Marques, R., Noronha, J. P., Mexia, J. T., Carvalho, G., Oehmen, A., & Reis, M. A. M. (2011). Assessing the diurnal variability

of pharmaceutical and personal care products in a full-scale activated sludge plant. *Environmental Pollution*, *159*(10), 2359–2367.

Schwarzenbach, R. P., Escher, B. I., Fenner, K., Hofstetter, T. B., Johnson, C. A., von Gunten, U., & Wehrli, B. (2006). The challenge of micropollutants in aquatic systems. *Science*, *313*(5790), 1072–1077.

Schwientek, M., Guillet, G., Rügner, H., Kuch, B., & Grathwohl, P. (2016). A high-precision sampling scheme to assess persistence and transport characteristics of micropollutants in rivers. *Science of the Total Environment*, *540*, 444–454.

Schwientek, M., Osenbrück, K., & Fleischer, M. (2013). Investigating hydrological drivers of nitrate export dynamics in two agricultural catchments in Germany using high-frequency data series. *Environmental Earth Sciences*, *69*, 381–393.

Selle, B., Schwientek, M., & Lischeid, G. (2013). Understanding processes governing water quality in catchments using principal component scores. *Journal of Hydrology*, *486*, 31–38.

Smith, A. J., Pollock, D. W., & Palmer, D. (2010). Groundwater interaction with surface drains in the Ord River Irrigation Area, northern Australia. Investigation by multiple methods. *Hydrogeology Journal*, *18*(5), 1235–1252.

Tomas, G., Hopker, R., Frigo, A. L., & Bleninger, T. (2016). Velocity mapping toolbox for SonTek M9 ADCP data. Conference paper: The International Conference on Fluvial Hydraulics, River Flow 2016, Iowa City, USA.

Twidale, C. (2004). River patterns and their meaning. *Earth-Science Reviews*, *67*(3–4), 159–218.

Ufrecht, W. (2002). Ein Hydrogeologisches Modell für den Karst- und Mineralwasseraquifer Muschelkalk im Großraum Stuttgart. Fachsektion Hydrogeologie der deutschen geologischen Gesellschaft (Ed.): *Hydrogeologische Modelle – ein Leitfaden mit Fallbeispielen. – Schriftreihe der Deutschen Geologischen Gesellschaft*, *Hydrogeologische* Beiträge 24, pp. 101–110; Hannover 2002.

Ufrecht, W. (2006). Hydrogeologie des Stuttgarter Mineralwassersystems. *Schriftenreihe des Amtes für Umweltschutz. 3/2006*. Stuttgart.

Unland, N. P., Cartwright, I., Andersen, M. S., Rau, G. C., Reed, J., Gilfedder, B. S., … Hofmann, H. (2013). Investigating the spatio-temporal variability in groundwater and surface water interactions. A multi-technique approach. *Hydrology and Earth System Sciences*, *17*(9), 3437–3453.

Villinger, E. (1982). Grundwasserbilanzen im Karstaquifer des Oberen Muschelkalks im Oberen Gäu (Baden-Württemberg). *Geologisches Jahrbuch*, *32*, 43–61.

Writer, J. H., Antweiler, R. C., Ferrer, I., Ryan, J. N., & Thurman, E. M. (2013). In-stream attenuation of neuro-active pharmaceuticals and their metabolites. *Environmental Science & Technology*, *47*(17), 9781–9790.

Yang, L., Song, X., Zhang, Y., Han, D., Zhang, B., & Long, D. (2012). Characterizing interactions between surface water and groundwater in the Jialu River Basin using major ion chemistry and stable isotopes. *Hydrology and Earth System Sciences*, *16*(11), 4265–4277.

Yu, M., L, C., Cartwright, I., Braden, J. L., & de Bree, S. T. (2013). Examining the spatial and temporal variation of groundwater inflows to a valley-to-floodplain river using 222Rn, geochemistry and river discharge. The Ovens River, southeast Australia. *Hydrology and Earth System Sciences.*, *17*(12), 4907–4924.

Zhao, D., Wang, G., Liao, F., Yang, N., Jiang, W., Guo, L., … Shi, Z. (2018). Groundwater-surface water interactions derived by hydrochemical and isotopic (^{222}Rn, deuterium, oxygen-18) tracers in the Nomhon area, Qaidam Basin, NW China. *Journal of Hydrology*, *565*, 650–661.

SUPPORTING INFORMATION

Additional supporting information may be found online in the Supporting Information section at the end of this article.

How to cite this article: Glaser C, Schwientek M, Junginger T, et al. Comparison of environmental tracers including organic micropollutants as groundwater exfiltration indicators into a small river of a karstic catchment. *Hydrological Processes*. 2020;34:4712–4726. https://doi.org/10.1002/hyp.13909